

## SUPPLEMENTAL MATERIAL

### Methods

Assessments of intracellular and global cholesterol homeostasis: Cell HDL binding was quantified using  $^{125}\text{I}$ -HDL<sup>1</sup> and protein measurements by the DC protein assay (Bio-Rad). Cell cholesterol efflux and selective uptake were also measured, using our previously-described methods<sup>1</sup>. In the latter approach, the efficiency of HDL COE (cholesteryl oleyl ether) selective uptake was further determined by subtracting values for vector-transfected cells and normalizing the amount of HDL COE selective uptake to the quantity of cell-associated HDL particles. SR-BI plasma membrane cholesterol binding was evaluated using [ $^3\text{H}$ ]-6-photocholesterol (American Radiolabeled Chemicals, Inc.) and our previously-reported approach<sup>2</sup>.

To assess global cholesterol homeostasis in mice, plasma total cholesterol was measured enzymatically (Infinity, Thermo Scientific, USA). For lipoprotein analysis, plasma samples pooled from two mice were subjected to fast protein liquid chromatography (FPLC) gel filtration using a Superose 6 column (GE Healthcare)<sup>3</sup>, and the cholesterol content of individual fractions was quantified.

Co-immunoprecipitation and immunoblotting: To evaluate the interactions between wild-type SR-BI versus SR-BI-Q445A and PDZK1<sub>HA</sub> in COS-M6 cells, co-immunoprecipitation was performed as described<sup>4</sup>. Polyclonal anti-SR-BI antibody against the extracellular domain or HA antibody was used for immunoprecipitation, and SR-BI C-terminal antibody or HA antibody for immunoblot analyses. A similar approach was used to evaluate SR-BI and c-Src interaction.

Immunoblot analyses, including for the evaluation of changes in eNOS Ser1179, c-Src Tyr416, and p38MAPK Thr180/Tyr182 phosphorylation, were performed using previously-described methods<sup>5, 6</sup>. Evaluations of wild-type SR-BI versus SR-BI-Q445A subcellular localization entailed plasma membrane preparations done as previously reported<sup>7</sup>, and caveolin-1 was used as a plasma membrane marker and  $\beta$ -actin as a cytoplasmic marker. Additional sucrose density gradient experiments were performed as previously described<sup>6</sup>. All findings for co-immunoprecipitation, sucrose gradient and immunoblotting studies were confirmed in at least 3 independent experiments.

eNOS activation and cell migration assays: eNOS activation was assessed by measuring [ $^{14}\text{C}$ ]-L-arginine to [ $^{14}\text{C}$ ]-L-citrulline conversion in intact cells as described previously<sup>8</sup>. All results were confirmed in at least 3 independent experiments.

Scratch assays were performed to assess endothelial cell migration<sup>9</sup>. Nontransfected or transfected cells were grown to near-confluence in 6-well plates, 24h later they were placed in DMEM media containing 1% charcoal/dextrin stripped FCS (Sigma) for 8h, and a defined region of cells was removed with a razorblade. Cell treatments then ensued for 24h at 37°C. Cells were fixed, and the number migrated past the wound edge was quantified per high power field.

Adenovirus generation and systemic administration: Wild-type SR-BI or SR-BI-Q445A cDNA was subcloned into pACCMVpLpA(-)loxP-SSP shuttle vector (<http://www2.med.umich.edu/medschool/vcore/PlasmidList.cfm>)<sup>10</sup>, and recombinant adenovirus was constructed by in vitro cre/loxP-mediated recombination<sup>11</sup>. Viruses were propagated in 911 cells, purified by centrifugation in CsCl gradients, and particles/ml were quantified by absorbance at 260nm. Adenovirus derived from empty shuttle vector (AdCMVpLpA-loxP, or AdNull) was used as a negative control for comparison with AdSR-BI and AdSR-BI-Q445A. Male C57BL/6 mice (8-10 weeks old) were injected via tail vein or jugular vein with  $1 \times 10^{11}$  particles of recombinant virus. In the studies of global cholesterol homeostasis, at baseline or 3 or 7d after adenovirus administration, blood was collected from the retro-orbital plexus after a 4 h-fast using heparinized capillary tubes. Venous injections and retro-orbital blood sampling were done under isoflurane anesthesia. Plasma was separated by centrifugation at 2000 X g for 30 min at 4°C for total cholesterol measurement or lipoprotein profile analysis<sup>12</sup>.

Macrophage reverse cholesterol transport (RCT): In vivo measurement of macrophage RCT was conducted using  $^3\text{H}$ -cholesterol-labeled foam cells as previously reported<sup>13</sup>. Briefly, 72h following systemic adenovirus administration by jugular vein injection as described above, mice received 500  $\mu\text{l}$  of a  $^3\text{H}$ -cholesterol-labeled foam cell suspension containing  $\sim 5 \times 10^6$  cells/ml at  $\sim 4.5 \times 10^6$  dpm/ml. To allow quantitative fecal collection, mice were housed individually on wire bottom cages for 48h with ad libitum access to food and water. At 6h and 24h post injection, blood was collected via the submandibular vein. At 48h post injection, mice were terminally anesthetized with ketamine/xylazine (100-160mg/kg ketamine-20-32mg/kg xylazine), and a midline laparotomy was performed. At necropsy blood was collected by heart puncture. Following blood collection, a whole body perfusion was conducted by puncturing the inferior vena cava and slowly delivering 10 ml of sterile 0.9% saline into the left ventricle of the heart to remove residual blood. Bile was collected from the gall bladder, and tissues were collected and snap frozen for subsequent analysis.

Immunofluorescence and confocal microscopy: Immunofluorescence and confocal analyses were performed in enterocytes as described<sup>6, 14</sup>. Briefly, cells were fixed with 4% paraformaldehyde and permeabilized with 0.1% saponin at 4°C; alexa fluor 568 phalloidin (F-actin labeling) was added at the same time as secondary antibodies to visualize the apical brush-border. Nuclei were stained with DAPI, and apoB was localized with primary anti-apoB (Chemicon) and secondary CY2 dye-labeled antibody (Molecular Probes). Immunofluorescence was examined by confocal fluorescence microscopy (LSM710 microscope Zeiss).

In vivo angiogenesis assays: HDL-induced angiogenesis was evaluated in vivo in mice using subcutaneously-placed 20  $\mu\text{l}$  silicone cylinders open at one end containing matrix and fibroblast growth factor-2 (0.5  $\mu\text{g}/\text{ml}$ ), with and without HDL added (100  $\mu\text{g}/\text{ml}$ ). The cylinders were harvested 14 days later and endothelial cell abundance in the defined volume of matrix was determined by staining the cells with FITC-lectin and quantification by fluorescence<sup>15, 16</sup>. To compare the impacts of expression of SR-BI versus SR-BI-Q445A, the adenoviral constructs encoding wild-type versus mutant receptor were introduced at the time of matrix preparation ( $2.5 \times 10^{11}$  particles/ml).

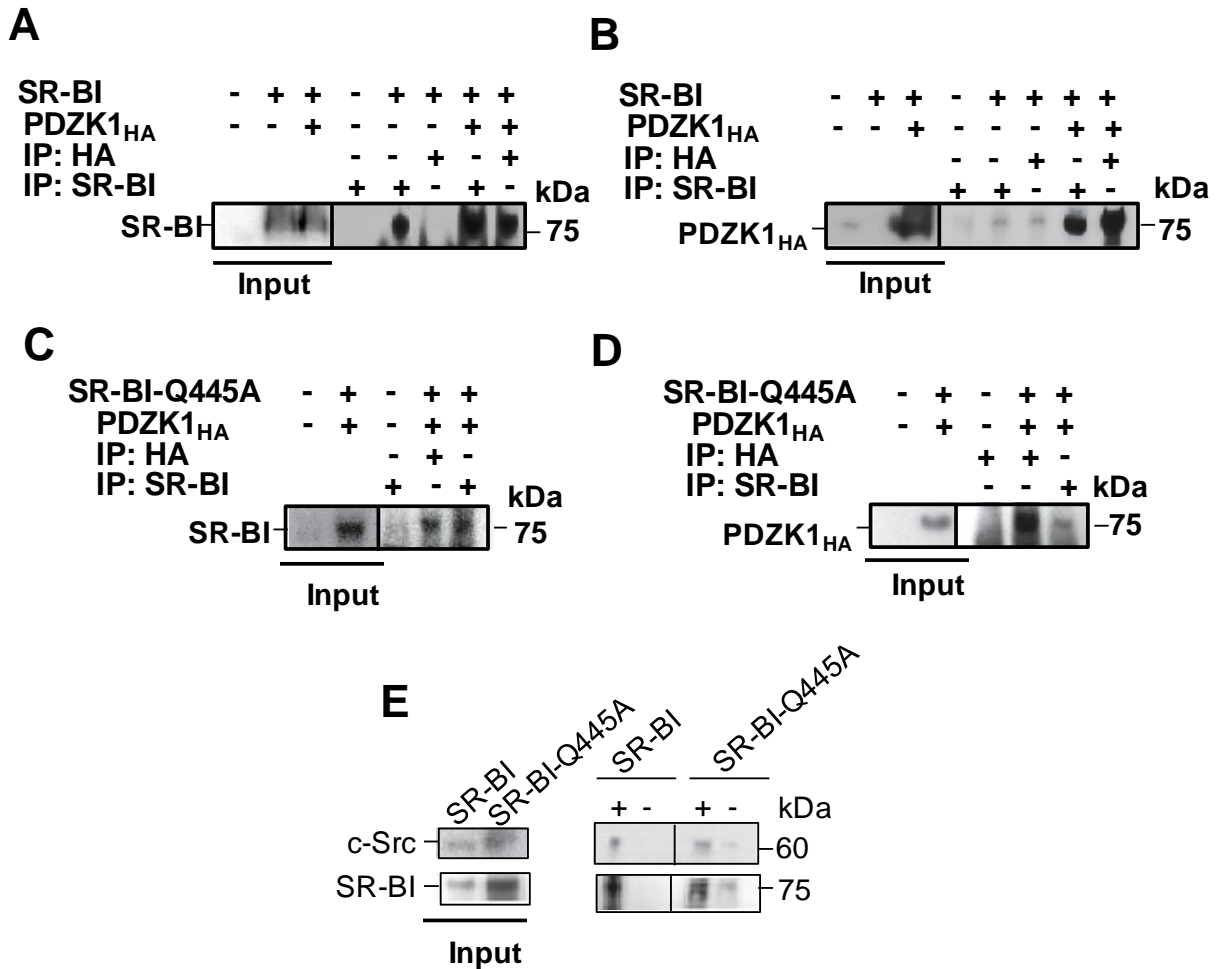
Statistical analysis: Differences between two groups were assessed by Student's t test, and differences between three or more groups were evaluated by analysis of variance (ANOVA) with Newman-Keuls post hoc testing. Values shown are mean $\pm$ SEM,  $p < 0.05$  was considered statistically significant.

## References

- (1) Connelly MA, Klein SM, Azhar S, Abumrad NA, Williams DL. Comparison of class B scavenger receptors, CD36 and scavenger receptor BI (SR-BI), shows that both receptors mediate high density lipoprotein-cholesterol ester selective uptake but SR-BI exhibits a unique enhancement of cholesterol ester uptake. *J Biol Chem* 1999;274:41-7.
- (2) Assanasen C, Mineo C, Seetharam D, Yuhanna IS, Marcel YL, Connelly MA, Williams DL, Llera-Moya M, Shaul PW, Silver DL. Cholesterol binding, efflux, and a PDZ-interacting domain of scavenger receptor-BI mediate HDL-initiated signaling. *J Clin Invest* 2005;115:969-77.
- (3) Kalaany NY, Gauthier KC, Zavacki AM, Mammen PP, Kitazume T, Peterson JA, Horton JD, Garry DJ, Bianco AC, Mangelsdorf DJ. LXRs regulate the balance between fat storage and oxidation. *Cell Metab* 2005;1:231-44.
- (4) Zhu W, Saddar S, Seetharam D, Chambliss KL, Longoria C, Silver DL, Yuhanna IS, Shaul PW, Mineo C. The Scavenger Receptor Class B Type I Adaptor Protein PDZK1 Maintains Endothelial Monolayer Integrity. *Circ Res* 2008;102:480-7.
- (5) Mineo C, Yuhanna IS, Quon MJ, Shaul PW. High density lipoprotein-induced endothelial nitric-oxide synthase activation is mediated by Akt and MAP kinases. *J Biol Chem* 2003;278:9142-9.
- (6) Beaslas O, Cueille C, Delers F, Chateau D, Chambaz J, Rousset M, Carriere V. Sensing of dietary lipids by enterocytes: a new role for SR-BI/CLA-1. *PLoS ONE* 2009;4:e4278.
- (7) Shaul PW, Smart EJ, Robinson LJ, German Z, Yuhanna IS, Ying Y, Anderson RG, Michel T. Acylation targets endothelial nitric-oxide synthase to plasmalemmal caveolae. *J Biol Chem* 1996;271:6518-22.
- (8) Yuhanna IS, Zhu Y, Cox BE, Hahner LD, Osborne-Lawrence S, Lu P, Marcel YL, Anderson RG, Mendelsohn ME, Hobbs HH, Shaul PW. High-density lipoprotein binding to scavenger receptor-BI activates endothelial nitric oxide synthase. *Nat Med* 2001;7:853-7.
- (9) Seetharam D, Mineo C, Gormley AK, Gibson LL, Vongpatanasin W, Chambliss KL, Hahner LD, Cummings ML, Kitchens RL, Marcel YL, Rader DJ, Shaul PW. High-density lipoprotein promotes endothelial cell migration and reendothelialization via scavenger receptor-B type I. *Circ Res* 2006;98:63-72.
- (10) Zeng X, Moore TA, Newstead MW, Hernandez-Alcoceba R, Tsai WC, Standiford TJ. Intrapulmonary expression of macrophage inflammatory protein 1alpha (CCL3) induces neutrophil and NK cell accumulation and stimulates innate immunity in murine bacterial pneumonia. *Infect Immun* 2003;71:1306-15.
- (11) Aoki K, Barker C, Danthinne X, Imperiale MJ, Nabel GJ. Efficient generation of recombinant adenoviral vectors by Cre-lox recombination in vitro. *Mol Med* 1999;5:224-31.
- (12) Kozarsky KF, Donahue MH, Rigotti A, Iqbal SN, Edelman ER, Krieger M. Overexpression of the HDL receptor SR-BI alters plasma HDL and bile cholesterol levels. *Nature* 1997;387:414-7.
- (13) Temel RE, Sawyer JK, Yu L, Lord C, Degirolamo C, McDaniel A, Marshall S, Wang N, Shah R, Rudel LL, Brown JM. Biliary sterol secretion is not required for macrophage reverse cholesterol transport. *Cell Metab* 2010;12:96-102.
- (14) Morel E, Demignot S, Chateau D, Chambaz J, Rousset M, Delers F. Lipid-dependent bidirectional traffic of apolipoprotein B in polarized enterocytes. *Mol Biol Cell* 2004;15:132-41.
- (15) Guedez L, Rivera AM, Salloum R, Miller ML, Diegmüller JJ, Bungay PM, Stetler-Stevenson WG. Quantitative assessment of angiogenic responses by the directed in vivo angiogenesis assay. *Am J Pathol* 2003;162:1431-9.

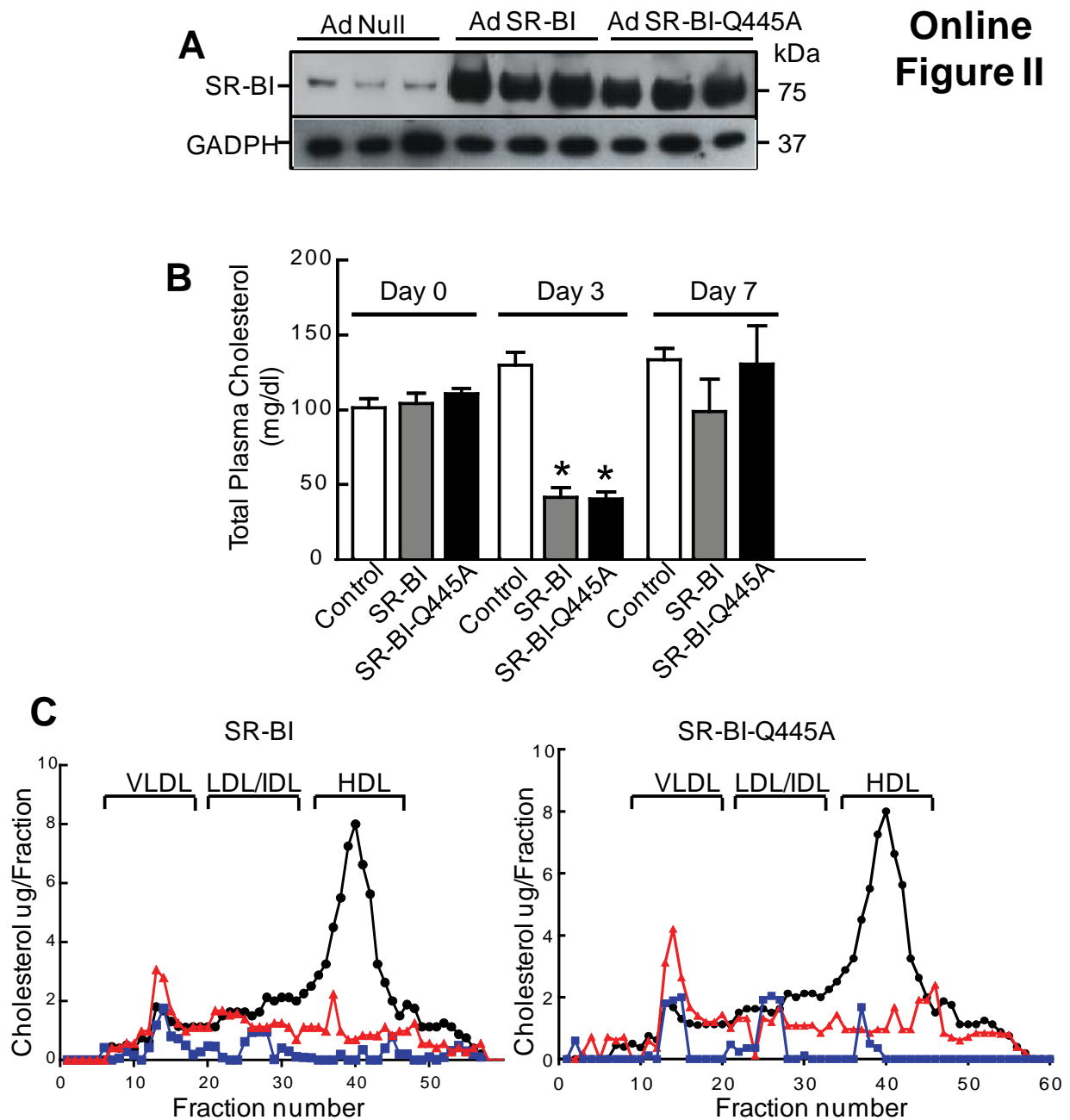
- (16) Koskimaki JE, Karagiannis ED, Tang BC, Hammers H, Watkins DN, Pili R, Popel AS. Pentastatin-1, a collagen IV derived 20-mer peptide, suppresses tumor growth in a small cell lung cancer xenograft model. *BMC Cancer* 2010;10:29.

# Online Figure I



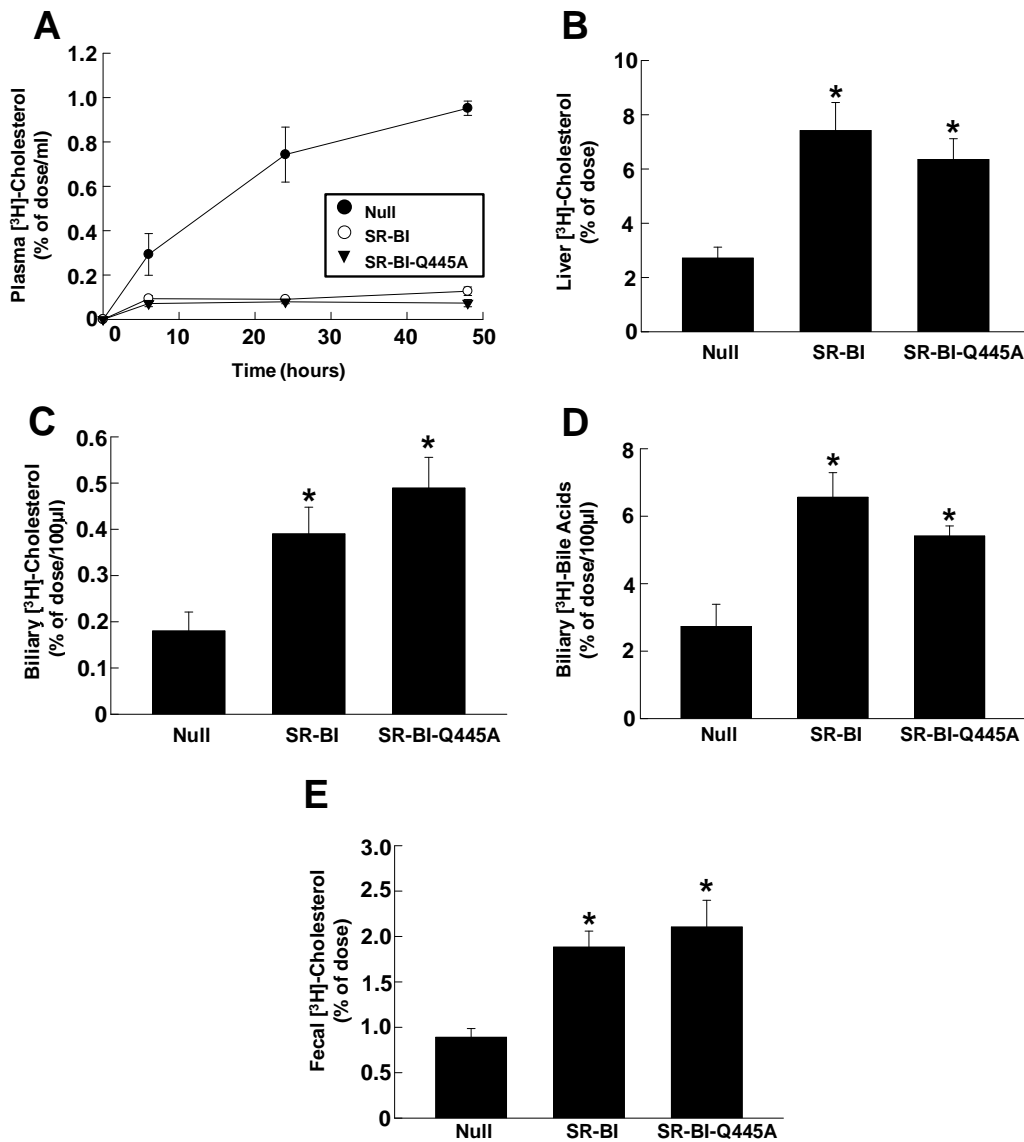
**Online Figure I:** SR-BI-Q445A interacts normally with PDZK1 and c-Src: (A, B) COS-M6 cells were cotransfected with sham plasmid or cDNAs encoding wild-type SR-BI and HA-tagged PDZK1 (PDZK1<sub>HA</sub>), and 48h later coimmunoprecipitations were performed using anti-SR-BI Ab or anti-HA Ab. Inputs are shown. Immunoprecipitations were immunoblotted for SR-BI (A) or HA (B). (C,D) In parallel experiments, cells were cotransfected with sham plasmid or cDNAs encoding SR-BI-Q445A and PDZK1 HA, coimmunoprecipitations were performed, and the immunoprecipitations were immunoblotted for SR-BI (C) or HA (D). (E) COS-M6 cells were transfected with cDNA encoding WT SR-BI or SR-BI-Q445A, and 24h later immunoprecipitations were performed on postnuclear supernatants with anti-SR-BI Ab directed to the extracellular domain (+ lane) or unrelated IgG control (- lane).

## Online Figure II



**Online Figure II:** Loss of SR-BI plasma membrane cholesterol sensing in liver does not alter global cholesterol homeostasis: (A) Male C57BL/6 mice were intravenously injected with either an empty control adenovirus (AdNull) or AdSR-BI or Ad-SR-BI-Q445A, and the abundance of receptor in the liver was evaluated 7d later by immunoblot analysis. Receptor abundance in 3 mice per group is shown. (B) Plasma cholesterol levels in the 3 study groups on days 0, 3 and 7. Values are mean $\pm$ SEM, n=10, \*p<0.05 vs AdNull control. (C) FPLC analysis of lipoproteins on days 0 (black), 3 (blue) and 7 (red) in mice that received AdSR-BI (left panel) or AdSR-BI-Q445A (right panel).

## Online Figure III



**Online Figure III:** Loss of SR-BI plasma membrane cholesterol sensing in liver does not alter macrophage RCT: Male C57BL/6 mice were intravenously injected with either an empty control adenovirus (Ad-Null) or Ad-SR-BI or Ad-SR-BI-Q445A, and 72h later they received a suspension of <sup>3</sup>H-cholesterol-labeled foam cells. Blood sampling and fecal collection were performed over a 48h period, and a terminal blood, bile and tissue harvest was then done. Plasma <sup>3</sup>H-cholesterol recovery (A), liver <sup>3</sup>H-cholesterol recovery (B), bile <sup>3</sup>H-cholesterol recovery (C), <sup>3</sup>H-bile acid secretion (D) and <sup>3</sup>H-cholesterol recovery in the feces (E) were quantified. Values are mean±SEM, n=8, \*p<0.05 vs Ad-Null.